Photophysics of Cyclic α-Diketone Aromatic Ring Bichromophoric Molecules. Structures, Spectra, and Intramolecular Electronic Energy Transfer

Sharona-Tal Levy, Mordecai B. Rubin, and Shammai Speiser*

Contribution from the Department of Chemistry, Technion—Israel Institute of Technology, Haifa 32000, Israel. *Received December 31, 1991*

Abstract: The structures and spectral properties of a number of bichromophoric molecules are presented. These bichromophoric molecules are composed of an aromatic ring connected by two methylene chains to an α-diketone moiety. Both absorption and emission spectra can be attributed to a superposition of the invididual spectra of the separate chromophores. The critical transfer radii for electronic energy transfer from the aromatic (donor) chromophore to the α-diketone (acceptor) chromophore were calculated from the spectral overlap between the fluorescence spectrum of the aromatic moiety and the absorption spectrum of the α-diketone chromophore. The results show that this series of molecules is well suited for a mechanistic study of short-range intramolecular electronic energy transfer (intra-EET). Results of singlet–singlet intra-EET in this series of bichromophoric molecules are reported. The temperature and molecular structure dependence of the intra-EET efficiency were measured and analyzed. The results show that the transfer efficiency is strongly temperature and structure dependent, indicating that exchange interaction is responsible for intra-EET between close chromophores in a bichromophoric molecule. The contributions of interchromophoric distance and of the relative orientation of the two chromophores to exchange interactions are discussed. Phosphorescence of the diketone moiety (including temperature dependence) was used to evaluate the efficiency of triplet energy transfer. Direct excitation of the diketone resulted in weak phosphorescence, indicating that intersystem crossing is inefficient. However, excitation of the aromatic moiety resulted in much more intense phosphorescence as a result of the formation of triplet diketone via triplet energy transfer. Complementarity between singlet and triplet energy transfer was evidenced by the fact that some compounds in which singlet energy transfer was more efficient exhibited weaker phosphorescence and vice versa. Quantitative correlations between triplet energy transfer efficiency and interchromophore distance were not possible.

1. Introduction

A bichromophoric molecule may be defined as a molecule built of two distinguishable molecular units connected by a molecular bridge. The properties of the bridge determine the flexibility of the whole bichromophoric structure. For a bichromophoric molecule, the electronic absorption spectrum can be described by a simple superposition of the absorption spectra of the two chromophores. The bridge serves as a molecular spacing unit which does not influence the basic electronic structure of the two chromophores while preventing intrachromophore interactions in the ground state. However, excitation of either chromophore may lead to such interactions and the observation of phenomena such as intramolecular complex formation,[1,2] intramolecular electron transfer, or intramolecular electronic energy transfer (intra-EET).[3-12]

In recent years, we have investigated several aspects of intra-EET. These studies involved the synthesis and characterization of specially designed bichromophoric molecules, shown in Figure 1. Study of these molecules enabled us to elucidate the mechanism of intra-EET for symmetrically linked bichromophoric molecules.[6-8]

Absorption spectra were recorded for these compounds together with the separate constituent chromophores. Most spectroscopic properties of the molecules were described by a superposition of those of their constituent chromophores. Unique for the bichromophoric molecules was the fact that, depending on the molecular geometry, energy absorbed by the aromatic chromophore was transferred in part to the α-diketone, and both chromophores emitted their fluorescence spectra.

Electronic energy transfer (EET) processes involve nonradiative transfer of electronic excitation from an excited donor molecule D* to an acceptor molecule A. The transfer may be an intermolecular process which can be described in terms of a bimolecular kinetic process[13]

$$D^* + A \xrightarrow{k_Q} D + A^* \quad (1)$$

where the bimolecular quenching process is related to an intermolecular energy transfer rate by

$$k_{ET}^{inter} = k_Q[A] \quad (2)$$

(1) De Schryver, F. C.; Boens, N.; Put, T. *Adv. Photochem.* **1977**, *10*, 359.
(2) Valeur, B. In *Fluorescence Biomolecules*; Jameson, D. M., Reinhardt, G. D., Eds.; Plenum Press: New York, 1969; p 296.
(3) (a) Weber, G. *Trans. Faraday Soc.* **1950**, *44*, 185. (b) Weber, G. *Nature* **1957**, *180*, 1409. (c) Weber, G.; Teale, F. W. J. *Trans. Faraday Soc.* **1958**, *54*, 640.
(4) Schnepp, O.; Levy, M. *J. Am. Chem. Soc.* **1962**, *84*, 172.
(5) (a) Lamola, A. A.; Leermakers, P. A.; Byers, G. W.; Hammond, G. S. *J. Am. Chem. Soc.* **1965**, *87*, 2322. (b) Lamola, A. A.; Hammond, G. S. *J. Chem. Phys.* **1965**, *43*, 2129. (c) Breen, D.; Keller, R. A. *J. Am. Chem. Soc.* **1968**, *90*, 1935. (d) Latt, S. A.; Cheung, H. T.; Blout, E. R. *J. Am. Chem. Soc.* **1968**, *90*, 6897. (e) Keller, R. A.; Dolby, L. Y. *J. Am. Chem. Soc.* **1969**, *91*, 1293. (f) Lamola, A. A. *J. Am. Chem. Soc.* **1969**, *91*, 4786. (g) Filipescu, N.; de Member, J. R.; Minn, F. L. *J. Am. Chem. Soc.* **1969**, *91*. (h) Bunting, J. B.; Filipescu, N. *J. Chem. Soc. B* **1970**, 1750. (i) Nairn, J. A.; Braun, C. L.; Caluwe, P.; Szwarc, M. *Chem. Phys. Lett.* **1978**, *54*, 469. (j) Zelent, B.; Messier, P.; Gauthier, S.; Gravel, D.; Durocher, G. *J. Photochem. Photobiol., A: Chem.* **1990**, *52*, 165. (k) Gravel, D.; Gauthier, S.; Brisse, F.; Raymond, S.; D'Amboise, M.; Messier, P.; Zelent, B.; Durocher, G. *Can. J. Chem.* **1990**, 908.
(6) (a) Speiser, S.; Katraro, R.; Welner, S.; Rubin, M. B. *Chem. Phys. Lett.* **1979**, *61*, 199. (b) Getz, D.; Ron, A.; Rubin, M. B.; Speiser, S. *J. Phys. Chem.* **1980**, *84*, 768.
(7) (a) Hassoon, S. *Photophysics and Photochemistry of Cyclic α-Diketones*. D.Sc. Thesis, Technion, Haifa, Israel, 1984. (b) Hassoon, S.; Lustig (Richter), H.; Rubin, M. B.; Speiser, S. *Chem. Phys. Lett.* **1983**, *98*, 345. (c) Speiser, S.; Katriel, J. *Chem. Phys. Lett.* **1983**, *102*, 88. (d) Hassoon, S.; Lustig, H.; Rubin, M. B.; Speiser, S. *J. Phys. Chem.* **1984**, *88*, 6367.
(8) Speiser, S.; Hassoon, S.; Rubin, M. B. *J. Chem. Phys.* **1986**, *90*, 5085.
(9) Zimmerman, H. E.; Goldman, T. D.; Hirzel, T. K.; Schmidt, S. P. *J. Org. Chem.* **1980**, *45*, 3934.
(10) Bourson, J.; Mugnier, J.; Valeur, B. *Chem. Phys. Lett.* **1982**, *92*, 430.
(11) (a) Oevring, H.; Verhoeven, J. W.; Paddon-Row, M. N.; Cotsaris, E. *Chem. Phys. Lett.* **1988**, *143*, 488. (b) Kroon, J.; Oliver, A. M.; Paddon-Row, M. N.; Verhoeven, J. W. *J. Am. Chem. Soc.* **1990**, *112*, 4868. (c) Amrein, W.; Schaffner, K. *Helv. Chim. Acta* **1975**, *58*, 397. (d) Wu, Z.; Morrison, H. *J. Am. Chem. Soc.* **1989**, *111*, 9267; **1992**, *114*, 4119. (e) Closs, G. L.; Johnson, M. D.; Miller, J. R.; Piotrowiak, P. *J. Am. Chem. SOc.* **1989**, *111*, 3751.
(12) (a) Ernsting, N. P.; Kaschke, M.; Kleinschmidt, J.; Drexhage, K. H.; Huth, V. *Chem. Phys.* **1988**, *122*, 431; *J. Phys. Chem.* **1990**, *94*, 5757. (b) Valeur, B.; Mugnier, J.; Pouget, J.; Bourson, J.; Santi, F. *J. Phys. Chem.* **1989**, *93*, 6073. (c) Osuka, A.; Maruyama, K.; Yamazaki, I.; Tamai, N. *J. Chem. Soc., Chem. Commun.* **1988**, 1243. (d) Osuka, A.; Maruyama, K. *J. Am. Chem. Soc.* **1988**, *110*, 4454. (e) Osuka, A.; Maruyama, K.; Yamazaki, I.; Tamai, N.; *Chem. Phys. Lett.* **1990**, *165*, 392.
(13) (a) Mataga, N.; Kubota, T. *Molecular Interactions and Electronic Spectra*; Dekker: New York, 1970. (b) Klafter, J.; Blumen, A. *J. Lumin.* **1985**, *34*, 77. (c) Klafter, J.; Blumen, A. *J. Chem. Phys.* **1986**, *84*, 1397. (d) Ali, M. A.; Ahmed, S. A. *J. Chem. Phys.* **1989**, *90*, 1984.

0002-7863/92/1514-10747$03.00/0

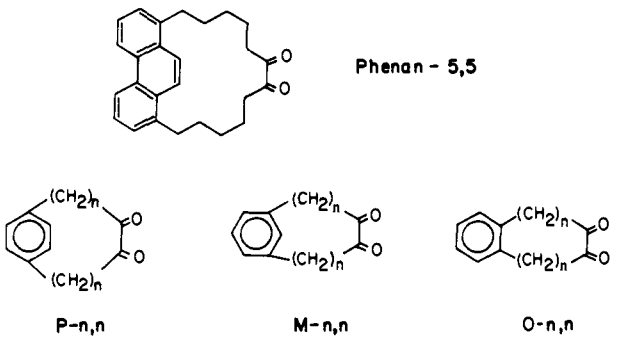

Figure 1. Structures of the bichromophoric molecules used for earlier studies of the interchromophoric distance dependence of intra-EET efficiency.[7,8]

Theoretically, k_{ET} is attributed to two possible contributions. The long-range Coulombic contribution formulated by Förster[14-16] in terms of dipole–dipole interaction is well documented.[16] It is particularly suitable for describing electronic energy transfer in solution whenever conditions for favorable spectroscopic overlap between the emission of D* and the absorption of A are met. The second contribution to EET can be realized whenever these conditions are not fulfilled. A short-range exchange interaction, as formulated by Dexter, can then facilitate EET.[18]

Intra-EET processes in bichromophoric molecules are usually described in terms of the process

$$D^*\text{-}(\ )\text{-}A \xrightarrow{k_{ET}^{ex}} D\text{-}(\ )\text{-}A^* \qquad (3)$$

where the excitation energy is transferred from an excited donor D* chromophore moiety to a ground-state acceptor moiety A, resulting in quenching of D* and sensitization of A; -( )- denotes a molecular spacer bridge connecting the two chromophores.

In all intra-EET processes discussed here, a resonance condition between the initial state of the system, D*-( )-A, and its final state, D-()-A*, is required. In solution, EET is slow compared to vibrational relaxation in D* and A*, the initial and final states are vibrationally relaxed, and the EET transitions are determined by the Frank–Condon principle at the common overlap frequencies of D and A.

Thus, EET is possible if the overlap integral

$$J = \int_0^\infty \bar{F}_D(\bar{\nu})\bar{\epsilon}_A(\bar{\nu})\, d\bar{\nu} \qquad (4)$$

is nonzero, where $\bar{F}_D(\bar{\nu})$ and $\bar{\epsilon}_A(\bar{\nu})$ are the normalized emission spectrum of D and the normalized extinction coefficient of A, respectively:

$$\int_0^\infty \bar{F}_D(\bar{\nu})\, d\bar{\nu} = \int_0^\infty \bar{\epsilon}_A(\bar{\nu})\, d\bar{\nu} = 1 \qquad (5)$$

The interactions leading to EET can be described by an interaction Hamiltonian and an interaction matrix element. When expanded in series, these are a combination of two terms. The first is the Coulombic contribution in the dipole–dipole interaction. The second is the exchange interaction, a quantum mechanical effect arising from the symmetry properties of the wave functions with respect to exchange of spin and space coordinates of two electrons in the D and A system.

The transfer rate k_{ET} for the first interaction is given by the Forster[14-16] relation for the long-distance dipole–dipole EET rate:

$$k_{ET}^{d-d} = \tau_D^{-1}(R_0/R)^6 \qquad (6)$$

where τ_D is the fluorescence decay time for D*, R is the distance between D and A, and R_0 is the critical transfer radius[14-16] given by $k_{ET}^{d-d} = 1/\tau_D$,

$$R_0^6 = \frac{9000(\ln 10)\kappa^2\phi_D}{128\pi^5 n^4 \tau_D} \int \frac{\bar{F}_D(\bar{\nu})\epsilon_A(\bar{\nu})\, d\bar{\nu}}{\bar{\nu}^4} \qquad (7)$$

where κ^2 is an orientation factor for the relative orientations of D and A dipoles, n is the refractive index of the medium, and ϕ_D is the fluorescence quantum yield of the donor.

The exchange interaction is expressed by the Dexter relation for short-range exchange interaction EET rate[18] constants:

$$k_{ET}^{ex} = (2\pi/\hbar)Z^2 \int F_D(E)F_A(E)\, dE = (2\pi/\hbar)Z^2 J_E \qquad (8)$$

where $F_D(E)$ and $F_A(E)$ are the normalized $F_D(\bar{\nu})$ and $\epsilon_A(\bar{\nu})$ in energy scale spectra and Z is the exchange integral expressing the spatial part of the exchange interaction matrix element, given by

$$Z = \int\int \phi_{D^*}(1)\phi_A(2)\frac{e^2}{r_{12}}\phi_D(2)\phi_{A^*}(1)\, d\tau_1\, d\tau_2 \qquad (9)$$

where r_{12} is the distance between electrons 1 and 2 which undergo exchange.

When D and A moieties are fixed in close proximity in a single bichromophoric molecule D–A and the interchromophore distance is shorter than the critical transfer radius R_0 for dipole–dipole interaction (eq 6), then intra-EET is governed by short-range interactions (eq 7). Taking hydrogen atom wave functions, Dexter approximated eq 8 by

$$k_{ET}^{ex} = (2\pi/\hbar)KJ \exp(-2R/L) \qquad (10)$$

where L is the average orbital radius involved in the initial and final states and K is a constant not related to experimental parameters.

It is useful to rewrite eq 10 in the form

$$k_{ET}^{ex} = (1/\tau_D)\exp[-\beta(R - R_0')] = \alpha \exp(-\beta R) \qquad (11)$$

where $\beta = 2/L$ and

$$\alpha = (2\pi/\hbar)Z^2 J_E = (2\pi/\hbar)KJ = \exp(\beta R_0'/\tau_D) \qquad (12)$$

Here R_0' is defined as R for which $k_{ET}^{ex} = (1/\tau_D)$; however, by contrast to R_0, R_0' cannot be calculated from measured spectra of D and A.

Since J involves *normalized* $\bar{\epsilon}_A(\bar{\nu})$ as opposed to $\epsilon_A(\bar{\nu})$ used to calculate R_0 for k_{ET}^{d-d} (eq 7), energy transfer via forbidden transitions in A is allowed by exchange interaction while they are much less probable in the Forster mechanism. Thus, we may conclude that unless $R_0 < 10$ Å, energy will be transferred mainly by the Forster mechanism.

Since the first investigations of intra-EET were reported by Weber et al.[3] and by Schnepp and Levy,[4] most workers in this field initially investigated molecules incorporating two chromophores connected by flexible chains and observed, irrespective of the exciting wavelength, emission only from the acceptor moiety: the quantum yield was independent of the length of the chain joining the donor and acceptor. In later work donor and acceptor groups were attached to rigid systems (such as steroids) so that their spatial relationship was known to a considerable degree but spatial variation was not possible, and in other cases the molecules were so flexible that spatial relationships could not be determined. The occurrence of intra-EET could readily be evaluated from knowledge of excitation and emission spectra of each moiety alone and comparison with spectra of the bichromophoric system.[5]

An ideal bichromophoric molecule suitable for study of the intra-EET process via short-range exchange interactions should have the following properties: (1) The molecular structure should be rigid enough to allow a limited number of molecular conformations. (2) Both absorption and emission spectra should reveal two bands, attributed to D or A chromophores. The general features of the spectra should be similar to a superposition of the separate spectra of the chromophores. (3) The value of J should be low as a result of poor spectral overlap between the emission

(14) Förster, Th. *Ann. Phys. (Leipzig)* **1948**, *2*, 55.
(15) Förster, Th. *Discuss. Faraday Soc.* **1959**, *27*, 7.
(16) Förster, Th. In *Modern Quantum Chemistry*; Istanbul Lectures; Sinanoglu, O., Ed.; Academic Press: New York, 1965.
(17) Speiser, S. *J. Photochem.* **1983**, *22*, 195.
(18) Dexter, D. L. *J. Chem. Phys.* **1953**, *21*, 836.
(19) Levy, S. T.; Speiser, S. *J. Chem. Phys.* **1992**, *96*, 3585.

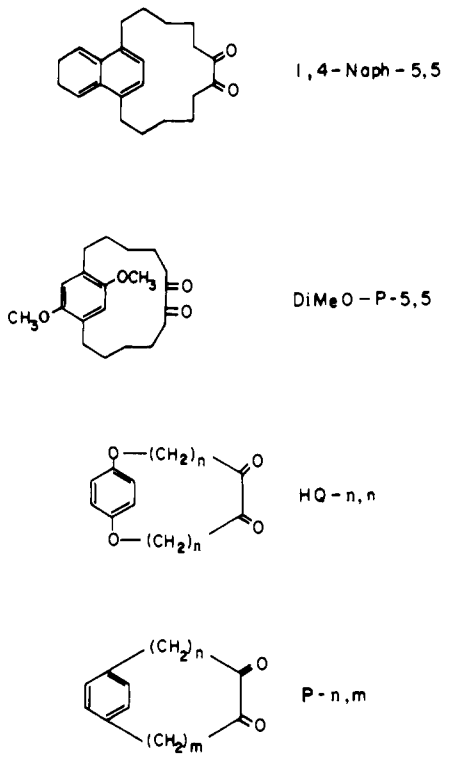

Figure 2. Structures of the bichromophoric molecules used for the present study of orientational and interchromophoric distance dependence of intra-EET efficiency.

of D* and the absorption of A. This will insure a negligible R_0 value indicative of inefficient dipole–dipole interactions and resulting in intra-EET which is controlled mainly by the exchange interaction. This requirement is further met by choosing an acceptor chromophore for which the A → A* transition is partially forbidden as manifested in a low ϵ_A value. As will be shown in this article, the series of molecules presented in Figure 2 meets the above requirements.

We[6-8] and others[5,9-12] have described bichromophoric systems which exhibit dual fluorescence due to partial intra-EET between D* and A. The first example of this behavior was a macrocyclic compound incorporating phenanthrene (D) and α-diketone (A) moieties, Phenan-5,5 (Figure 1). Subsequently, the compounds shown in Figure 1 incorporating the α-diketone (A) and a disubstituted benzene ring (D) were studied. Dual fluorescence was also observed in the case of intra-EET in aryl monoketones where evidence for through-bond interactions was provided[11b,d,e] and where the relationship to intramolecular electron transfer was discussed.[11e]

The series of molecules in Figure 1 was designed with the expectation that variation of the number of methylene groups in each chain joining the two chromophores would result in variation of the distance separating them and allow evaluation of the dependence of intra-EET efficiency on distance. Conformations of these molecules were determined by a combination of spectroscopic analysis (UV–vis, variable-temperature NMR), X-ray crystallography (where applicable), and molecular mechanics calculations.[9] Most spectroscopic properties of these molecules are described by a superposition of those of their constituent chromophores. Unique for the bichromophoric molecule is the fact that, depending on the molecular geometry, energy absorbed by the aromatic chromophore (at 266 nm) is transferred in part to the α-diketone and both chromophores emit their characteristic fluorescence spectra. An extensive study was made of the singlet–singlet (S–S) intra-EET process in solution as a function of temperature. Analysis of the results indicated that intra-EET involved the Dexter exchange mechanism.[7]

The earlier results obtained with these compounds showed that cyclic α-diketones incorporating an aromatic ring are excellent substrates for studies of intra-ET because of the minimal value of $J(2 \times 10^{-7})$ in these systems. The key factors from the experimental point of view are the combination of (1) minimal overlap in absorption spectra of the two chromophores so that selective excitation of either is possible and (2) minimal overlap in emission spectra of each so that the contribution of each chromophore to the emission spectra of the entire molecule can be evaluated. These conditions are met for both singlet–singlet (S–S)[7] and triplet–triplet (T–T) intra-EET.[8]

These earlier studies of intra-EET in bichromophoric molecules established the dependence of the intra-EET efficiency on the average interchromophore distance $\bar{R}$. This was valid mainly because the molecular geometry was that of symmetric bichromophoric molecules in which the relative orientation of the two chromophores remained the same for all $\bar{R}$ values within a given series.

Since the exchange interaction (eq 8) involves the actual spatial overlap of the molecular orbitals of the two interacting chromophores, the relative orientation should have a significant effect on the intra-EET efficiency. Such studies of orientational effects are described in the present article.

For this purpose the series of bichromophoric molecules, depicted in Figure 2, was synthesized. In this article we first provide the spectroscopic and calculated structural data for these molecules as a basis for the investigation of the mechanisms of singlet–singlet intra-EET and triplet–triplet intra-EET. A detailed mechanistic study of singlet–singlet and triplet–triplet intra-EET is also discussed here.

2. Experimental Section

2.1 Synthesis. The general synthetic approach involved synthesis of diesters which underwent cyclization to acyloins followed by oxidation to diketones, as described previously.[20] The acyloin cyclization failed with dimethyl catechol dipropionate and dimethyl hydroquinone divalerate.

2.2 Structure Analysis and Spectral Data. The molecular geometry was determined using MacroModel (version 3.0) software with an MM-2 force field with special parameters for α-diketones.[21]

Melting points are uncorrected. Infrared spectra of liquids were determined on liquid films and spectra of solids in potassium bromide pellets. NMR spectra were determined in deuteriochloroform solutions at 60 or 400 MHz. Mass spectra were determined using an ionizing current of 70 eV. Thin-layer chromatography was performed using silica gel plates.

HQ-66 diketone: mp 60–1 °C (hexane); ^{1}H NMR (400 MHz) δ 6.79 (4 H), 4.05 (t, J = 5.6, 4 H, C-1), 2.45 (t, J = 7.2, 4 H, C-6), 1.62 (m, 4 H, C-2), 1.41 (m, 8 H, C-3 and C-5), 1.24 (m, 4 H, C-4) (small coupling of ArH to C-1H COSY suggests weak coupling of benzylic and aromatic protons); MS m/e 332.1967 (−2.0, 95), 100 $C_6H_6O_2$, $C_{20}H_{28}O_4$ requires 332.1980.

HQ-5,5 diketone: ^{1}H NMR (400 MHz) δ 6.77 (4 H), 4.13 (t, J = 6.5, 4 H, C-1), 2.43 (t, J = 6.5, 4 H, C-5), 1.5–1.59 (m, 8 H, C-2 and C-4), 1.30 (pent, J = 7, 4 H, C-3); MS m/e 304.1725 (5.0, 92), 110.0275 (−9.2, 100), $C_{18}H_{24}O_4$ requires 304.1688.

P-5,5 (from previous work): ^{1}H NMR (400 MHz) δ 6.99 (4 H), 2.59 (t, J = 5, 4 H, benzylic hydrogens, C-1), 2.37 (t, J = 7, 4 H, α to CO, C-5), 1.58 (m, 4 H, C-2), 1.24 (m, 4 H, C-4), 1.03 (M, 4 H, C-3); ^{13}C NMR 200.0, 139.63, 128.74, 35.11, 29.56, 27.11, 23.50 ppm.

P-6,4 diketone: oil, crystallized in refrigeration; IR (CHF) 1720 cm^{-1}; λ_{max} 425 (19); ^{1}H NMR (400 MHz) δ 7.01 (m, 4 H), 2.57 (m, 4 H, benzylic), 2.36 (t, J = 6.7, 2 H, 4 or 6), 2.18 (t, J = 6.8, 2 H, other α), 1.54 (m, 4 H), 1.43 (m, J = 6.7, 2 H), 1.35 (pent, J = 6.7, 2 H), 1.02 (m, 4 H); MS m/e 272.1748 (100), $C_{18}H_{24}O_2$ requires 272.1769.

P-7,3 diketone: oil, crystallized in refrigeration; IR (CHF) 1705 cm^{-1}; λ_{max} 425 (23); ^{1}H NMR (400 MHz) δ 7.01 (m, 4 H), 2.64 (m, 4 H, benzylic), 2.58 (m, 2 H), 1.98 (t, J = 7, 2 H), 1.63 (m, 2 H), 1.1–1.4 (m, 8 H) ppm.

P-8,2 diketone: oil, crystallized in refrigeration; IR (CHF) 1705 cm^{-1}; ^{1}H NMR (400 MHz) δ 7.03 (4 H), 3.05 (m, 2 H, benzylic), 2.99 (m, 2 H), 2.56 (m, 2 H), 2.33 (t, J = 7, 2 H), 1.59 (m, 2 H), 1.10 (m, 2 H), 0.97 (m, 8 H).

DiMeO-P-5,5: mp 104–6 °C; ^{13}C NMR 200.40, 151.28, 128.63, 113.62, 56.09, 35.02, 39.72, 27.76, 23.59 ppm; MS m/e 332.1980 (100), 304.2113 (19, M^+ − CO), $C_{20}H_{28}O_4$ requires 332.1980.

(20) Rubin, M. B.; Migdal, S.; Speiser, S.; Kaftory, M. *Isr. J. Chem.* **1985**, *25*, 66.

(21) Isaksson, R.; Liljefors, T. *J. Chem. Soc., Perkin Trans. 2* **1983**, 1351.

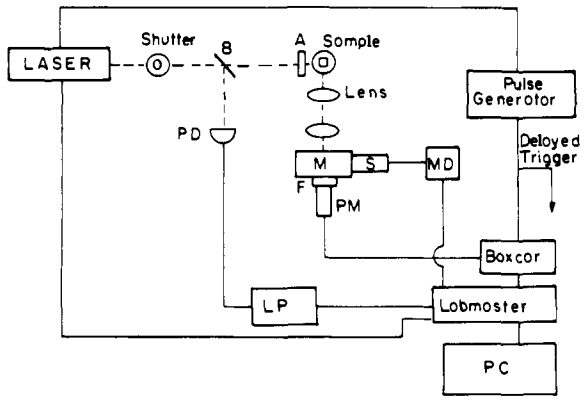

Figure 3. Experimental setup for measuring time-resolved fluorescence and phosphorescence spectra: B, beam splitter; PD, photodiode; LP, laser photometer; A, attenuator; M, monochromator; L, filter; S, stepper motor; PM, photomultiplier; MD, motor drive; PC, personal computer.

2.3 Sample Preparation. The bichromophoric compounds were dissolved in a 1:1 mixture of methylcyclohexane (MCH) and isopentane (*i*-P); both solvents were of spectrograde quality and were dried on basic alumina. Models for the separate chromophores were *p*-xylene, hydroquinone dimethyl ether, 1,4-dimethylnaphthalene, and biacetyl. Samples were degassed by freeze–pump–thaw cycles.

2.4 Absorption Spectra. Absorption spectra were recorded using a Hewlett-Packard 8452A diode array spectrophotometer.

2.5 Fluorescence Spectra. Corrected fluorescence spectra were recorded with a Shimadzu RF-540 spectrofluorimeter. For temperature-dependent spectra a stainless steel optical dewar equipped with quartz windows was used. An IBM personal computer was used for controlling the fluorimeter as well as for data acquisition and data analysis.

2.6 Time-Resolved Emission Spectra. The experimental setup employed for studies of time-resolved temperature-dependent emission spectroscopy of the bichromophoric molecules is depicted in Figure 3.

Excitation was provided by a Quanta-Ray PDL-1 dye laser pumped by a Quanta Ray DCR-10 ND-YAG laser and its harmonic generated frequencies. The α-diketone was excited at 430 nm obtained by pumping Coumarin-440 dye solution. For excitation of the aromatic moiety, a 266-nm quadrupled Nd-YAG beam was used. The laser repetition rate was 10 Hz. The laser as well as the data acquisition system was controlled by an IBM personal computer using Asyst software and a Labmaster control card. Signals from a Hamamatsu R777 photomultiplier were fed into either a Molectron LP20 photometer or a PAR 162/164 boxcar. The photomultiplier was attached to a Bausch and Lomb high-intensity monochromator equipped with a stepping motor also controlled by the computer. According to the specific time resolution needed (fluorescence or phosphorescence recording), the sampling gating time Δ and the sampling duration δ were determined. Corrections for variations in the laser pump intensity were made using the reference signal of a Molectron 141 photodiode.

3. Results

3.1 Molecular Structure. Our goal in the present study was to find the correlation between molecular structure and the intra-EET process. This requires detailed information on the molecular geometry. X-ray crystallography could be performed only on P-4,4. Comparison with the results of molecular mechanics calculations showed very good agreement between the two methods.[20] Therefore, molecular mechanics calculations were used for all other molecules.

Calculated[22] stereographic projections of the molecules at directions perpendicular and parallel to the aromatic ring show that in all compounds the bridge methylene chains are in a staggered conformation. For all molecules we find that lengthening the bridge increases R. For the symmetric structures the center of the intercarbonyl bond lies above that of the aromatic ring.

In order to calculate the exchange interaction[19] we have represented the location of the α-diketone plane relative to that of the aromatic ring by two matrices. The first is a translation matrix of the aromatic ring center with respect to the center of the intercarbonyl bond, while the second describes the relative rotation of the two planes (see Figure 4). In spherical coordinates this

(22) Levy, S. T. M.Sc. Thesis, Technion, Haifa, Israel, 1991.

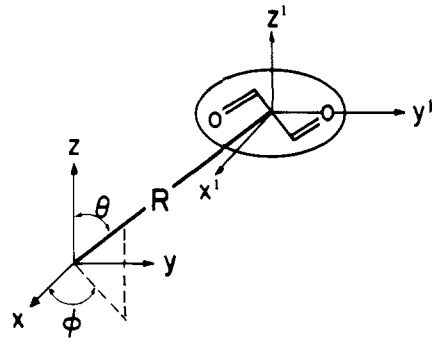

Figure 4. Description of the parameters in the translation matrix of the center of the α-diketone in the aromatic ring (x, y, z) coordinate system. R is the distance between the centers of the two chromophores; θ' and ϕ' are the azimuthal angles.

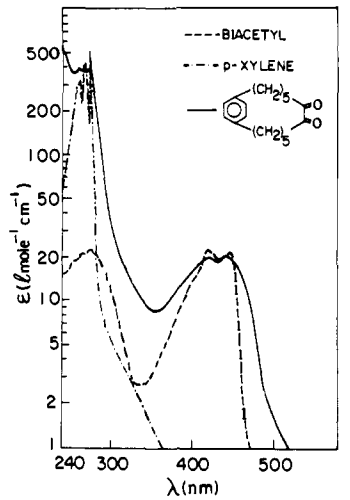

Figure 5. Absorption spectrum of the bichomophoric molecule P-5,5 (—) together with the corresponding spectra for *p*-xylene (···) and biacetyl (- - -) dissolved in MCH and *i*-P (1:1).

Table I. Translation Matrix in Spherical Coordinates of the α-Diketone Plane Center in Relation to the Center of the Aromatic Ring for the Bichromophoric Molecules

molecule	R (Å)	θ'	ϕ'
P-5,5	5.252	0.578	0.541
P-6,4	4.766	29.4	61.28
P-7,3	5.049	27.0	66.3
P-8,2	4.06	40.7	77.5
HQ-5,5	4.93	0.2	68.6
HQ-6,6	6.98	0.8	32.8
DiMeO-P-5,5	5.22	0.2	17.7
1,4-Naph-5,5	5.23	4.2	46.5

matrix shows the difference between the symmetric molecules and the asymmetric ones where θ' represents the deviation from perfect symmetry at 0°. The results[19] are summarized in Table I. It is evident that except for the P-n,m series ($n \neq m$) all structures are close to the symmetric configuration. Our conclusion is that these series of molecules can serve for the investigation of structural effects on intra-EET which is described below.

3.2 Absorption Spectra. Compounds belonging to a particular series exhibit similar spectra consisting of two principal absorption bands. By comparing these spectra with those obtained for the separate corresponding chromophores, we conclude that these spectra are indeed a superposition of the spectra of the two chromophores. Shifts from the positions of the separate chromophores can be attributed to the particular molecular conformation. The α-diketone band in all compounds appears in the 430–445-nm spectral region with extinction coefficients of 10–25 L mol^{-1} cm^{-1}, typical of α-diketones. An example is shown in Figure 5 for P-5,5; other absorption spectra are summarized in Table II together with data on the fluorescence spectra discussed

Table II. Spectral Features of the Bichromophoric Molecules and Their Constituent Chromophores

molecule	absorption $\lambda(D)_{max}$ (nm)	$\epsilon(D)$ (cm^{-1} M^{-1})	$\lambda(A)_{max}$ (nm)	$\epsilon(A)$ (cm^{-1} M^{-1})	emission $\lambda(D)_{max}$ (nm)	$\lambda(A)_{max}$ (nm)
biacetyl			420	15 ± 4		462
p-xylene	266	980 ± 80			298	
P-5,5	266	380 ± 40	440	25 ± 5	294	481
P-6,4	266	1200 ± 100	430	9 ± 3	291	487
P-7,3	266	650 ± 50	428	9 ± 3	295	478
P-8,2	264	840 ± 60	438	9 ± 3	298	487
HDME[a]	288	320 ± 40			317	
HQ-5,5	290	2600 ± 300	430	24 ± 6	322	483
HQ-6,6	292	1000 ± 100	440	12 ± 4	323	482
DiMeO-P-5,5	294	4200 ± 500	438	23 ± 6	324	481
1,4-DMN[b]	289	7700 ± 600			341	
1,4-Naph-5,5	282	5900 ± 600	444	17 ± 5	339	490

[a] Hydroquinone dimethyl ether. [b] 1,4-Dimethylnaphthalene.

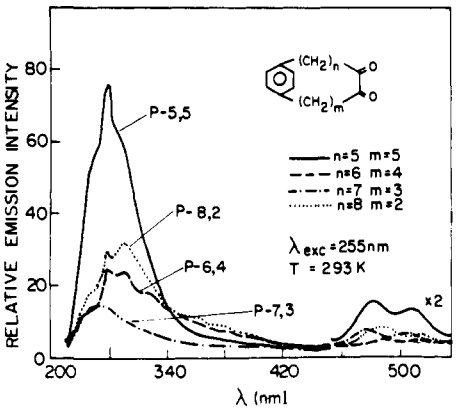

Figure 6. Fluorescence spectra of the four bichromophoric molecules of the series P-*n,m* dissolved in MCH and *i*-P (1:1), excited at 255 nm at room temperature and normalized for absorption.

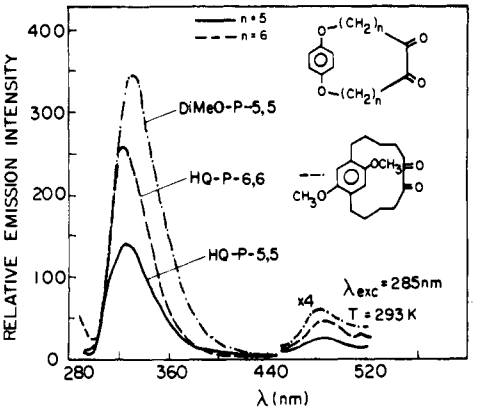

Figure 7. Fluorescence spectra for the bichromophoric molecule P-7,3 excited by 255 nm, at two temperatures.

in the next section. The difference in the positions of the maxima for the α-diketone bands can be attributed to differences in the dihedral angle between the two carbonyls.[23] The second absorption band appears at shorter wavelengths with much higher intensity and corresponds to the aromatic moiety absorption (see Table II). Since previous work has shown insignificant variation of the absorption spectra with temperature,[7,11] we report only room-temperature data.

3.3 Fluorescence Emission Spectra. The basic singlet–singlet intra-EET experiment consisted of measuring the temperature-dependent fluorescence quantum yield of the aromatic moiety emission. All bichromophoric samples show dual fluorescence; the emission band centered around 300 nm is attributed to emission from the excited aromatic chromophore. The quantum yield of this emission is indicative of the efficiency of intra-EET to the α-diketone chromophore. The transfer efficiency can be determined from the temperature and molecular structure dependence of the donors' fluorescence quantum yields. The fluorescence spectra for the P-*n,m* bichromophoric molecules are shown in Figure 6. Similar spectra were obtained for all other bichromophoric molecules, and their main features are given in Table II. These spectra were obtained for excitation at 255 nm for P-*n,m* and 1,4-Naph-5,5 and at 285 nm for the HQ-*n,n* molecules. All of these corrected spectra were normalized for variations in absorption at the excitation wavelengths. Since the aromatic chromophore absorbs about 25 times more strongly than the α-diketone (Figure 5), the residual emission from the α-diketone moiety upon UV excitation can be neglected. These spectra are indicative of the molecular structure dependence of the intra-EET process.

An example of the temperature-dependent fluorescence spectra of the aromatic chromophore for P-7,3 is shown in Figure 7 for the two extreme temperatures employed. Similar results[22] were obtained for all other bichromorphic molecules. The relative fluorescence quantum yield of the donor chromophore, ϕ, can be determined from the integrated band intensity. The results for P-7,3 are shown in Figure 8, together with a fit to a kinetic model for temperature-dependent intra-EET described in the Discussion. Tables III and IV summarize the temperature-dependent measurements for all bichromophoric molecules.

Table III. Experimental Singlet–Singlet Intra-EET Quantum Yields, ΔE Values, and Calculated[19] Average Interchromophore Distances

molecule	λ_{exc} (nm)	Q	$\bar{R}$ (Å)[19]	ΔE (cm^{-1})
P-4,4	255	0.99[7]	3.25	∞[7]
P-5,5	255	0.84	5.25	1790
P-6,6	255	0.74[7]	5.40	∞[7]
P-6,4	255	0.915	4.77	980
P-7,3	255	0.964	5.05	1010
P-8,2	255	0.907	4.06	1400
M-3,3	255	0.84[7]	5.10	1154[7]
M-4,4	255	0.91[7]	4.12	1715[7]
O-3,3	255	0.23[7]	4.50	∞[7]
O-4,4	255	0.02[7]	6.00	1260[7]
HQ-5,5	285	0.94	4.93	1600
HQ-6,6	285	0.903	6.98	2550
DiMeO-P-5,5	285	0.846	5.22	1400
1,4-Naph-5,5	255	0.925	5.23	1190
Phenan-5,5	377	0.23[6]	5.75[6]	600[6]

Table IV. ΔE Values for Bichromophoric Molecules with Similar Methylene Bridges and Different Spectral Overlap Integrals

molecule	ΔE (cm^{-1})	J' (cm × 10^8)	$\bar{R}$ (Å)[19]
P-5,5	1790 ± 30	1.2	5.25
HQ-5,5	1590 ± 100	3.9	4.93
1,4-Naph-5,5	1190 ± 70	10.0	5.23

3.4 Energy Transfer Parameters. The absorption and emission spectra of all bichromophoric molecules meet the basic requirements for intra-EET studies as discussed in the Introduction. Both

(23) (a) Leonard, N. J.; Mader, P. M. *J. Am. Chem. Soc.* **1950**, *72*, 5388. (b) Verheijdt, P. L.; Cerfontain, H. *J. Chem. Soc., Perkin Trans. 2* **1983**, 1343.

(24) Li, F.; Lee, J.; Bernstein, E. R. *J. Phys. Chem.* **1983**, *87*, 254.

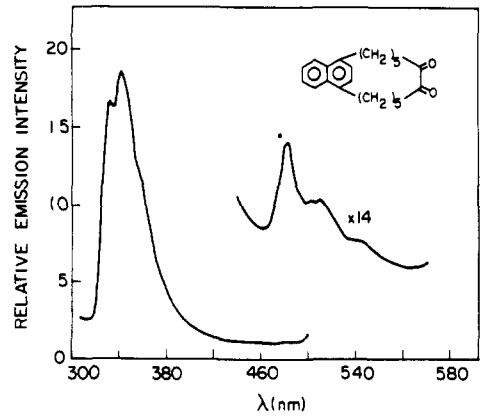

Figure 8. Temperature-dependent relative fluorescence quantum yield ϕ for the aromatic chromophore of the bichromophoric molecule P-7,3 together with the line fitted to eq 14.

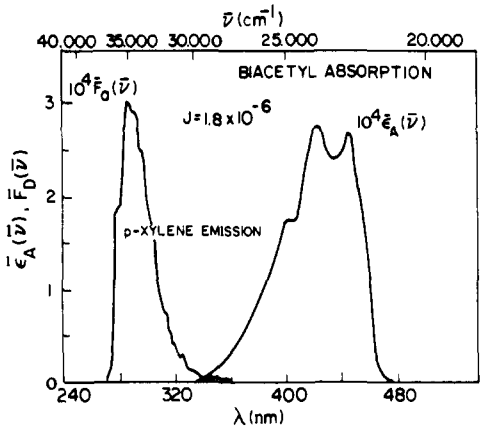

Figure 9. Normalized fluorescence spectrum of *p*-xylene at 255-nm excitation and the normalized absorption spectrum of biacetyl.

Table V. Spectral Overlap Integral, J', for Dipole–Dipole Interactions and Critical Radii, R_0, for the Bichromophoric Molecules

acceptor chromophore	donor chromophore	R_0 (Å)	J' (cm × 10^8)
biacetyl	*p*-xylene		
	P-5,5	4.9	1.2
	P-6,4	5.1	1.5
	P-7,3	4.9	1.3
	P-8,2	5.3	1.7
biacetyl	hydroquinone dimethyl ether		
	HQ-5,5	5.2	3.9
	HQ-6,6	5.0	2.9
	DiMeO-P-5,5	5.1	3.2
biacetyl	naphthalene		
	1,4-Naph-5,5	6.9	10.0

spectra can be obtained by a simple superposition of the corresponding spectra of the separate moieties. The extent of spectral overlap for the donor and acceptor moieties and the resulting value of the overlap integral J' are shown in Figure 9 for xylene and biacetyl. The corresponding results for all of the bichromophoric molecules are summarized in Table V together with the Förster critical radius R_0 calculated from eq 7. The small R_0 values which are comparable to the interchromophoric distances (Table I) mean that the dipole–dipole interaction is weak compared to the exchange interaction for all molecules.

We may thus conclude that the bichromophoric molecules chosen for this study are suitable for investigation of the intra-EET process proceeding by short-range exchange interactions.

3.5 Phosphorescence Spectra. Time-resolved fluorescence and phosphorescence of P-5,5 excited at 266 nm (aromatic ring absorption) are shown in Figure 10. Time-resolved fluorescence and phosphorescence of P-5,5 excited at 430 nm (α-diketone

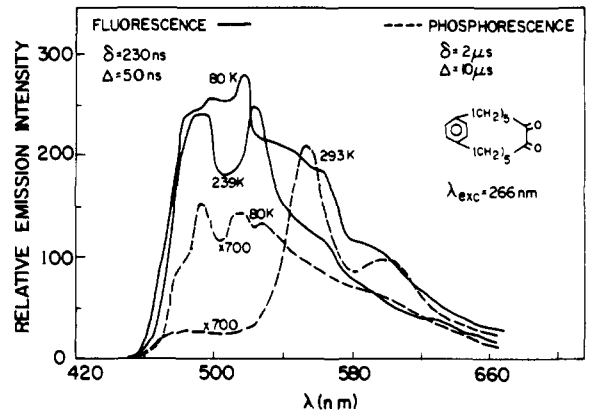

Figure 10. Temperature-dependent time-resolved fluorescence (—) and phosphorescence (---) spectra of P-5,5 excited at the aromatic ring absorption band (266 nm).

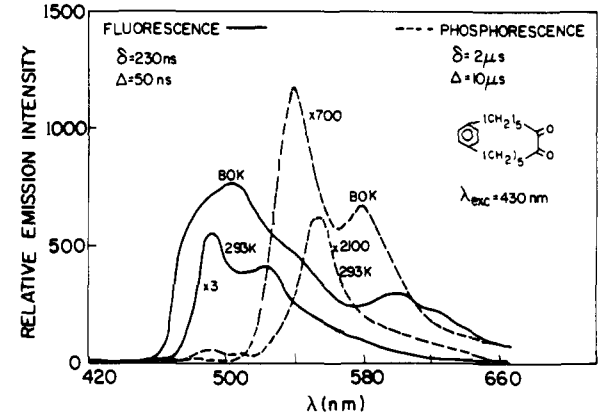

Figure 11. Temperature-dependent time-resolved fluorescence (—) and phosphorescence (---) spectra of P-5,5 excited at the α-diketone absorption band (430 nm).

absorption) are shown in Figure 11, showing different phosphorescence yields as compared to the 266-nm excitation. For all bichromophoric molecules α-diketone phosphorescence is observed, again with different yields depending on the particular excitation band.[22]

The fluorescence and phosphorescence quantum yields for all of the bichromophoric molecules of Figure 2 excited at the α-diketone absorption band (430 mn) and at the aromatic moiety absorption band (266 nm) at 293 and 80 K are summarized in Table VI.

4. Discussion

In a previous study[7] we examined the fluorescence spectra of an equimolar mixture of *p*-xylene and biacetyl induced by exciting *p*-xylene at 260 nm. The spectrum showed two emission bands, one attributed to *p*-xylene and the other to biacetyl. The biacetyl band is indicative of a collisional EET process and disappears when the solution is frozen so as to eliminate collisions.

The spectral overlap measurements show that intra-EET between aromatic and α-diketone moieties are controlled by exchange interaction. In order to account for the observed molecular structural dependence of the intra-EET and the observed temperature dependence, we developed a model for exchange interaction controlled, short-range intra-EET in bichromophoric molecules.

In this model we treat the temperature dependence kinetically and complement it by calculating the average intra-EET efficiency for a distribution of bichromophoric molecular conformers in order to account for the distance and orientation dependence of the transfer yield. In addition, the observed yield is compared to the calculated exchange integral.[20]

4.1 The Kinetic Model for Singlet–Singlet Intra-EET. Our previous results on intra-EET indicated the existence of several conformations for the bichromophoric molecules.[7] Since con-

Table VI. Relative Corrected Fluorescence and Phosphorescence Quantum Yields for the α-Diketone Chromophore of the Bichromophoric Molecules

		λ_{exc} = 266 nm			λ_{exc} = 430 nm			
molecule	T (K)	$\phi_{ET}^{F}(A)$	$\phi_{ET}^{P}(A)$	$10^4\rho_{ET}$	$\phi_{d}^{F}(A)$	$\phi_{d}^{P}(A)$	$10^4\rho_{d}$	ξ^{T-T}
P-4,4[8]	123	943.7	4.78	50.6	297	0.293	9.9	5.11
P-5,5	293	624.5	0.608	9.74	1322	0.552	4.18	2.33
	80	250.6	0.752	30.0	2416	3.19	13.2	2.27
P-6,6[8]	123	3500	0.391	1.1	3.09	0.122	1.1	1.0
P-6,4	293	1224	0.338	2.76	4454	0.871	1.96	1.41
	80	1791	3.26	18.2	7883	4.62	5.86	3.10
P-7,3	293	899.6	0.427	4.75	2223	1.21	5.44	0.873
	283	688.8	0.417	6.24	1219	1.09	8.92	0.699
	269	266.5	0.375	14.1	1130	1.39	12.3	1.15
	242	435.8	0.498	11.4	1211	2.98	24.6	0.464
	185	374.3	0.600	16.0	1251	3.56	28.5	0.563
	136	190.0	0.562	29.6	1148	3.81	26.3	1.13
	80	952.0	1.063	11.2	3615	3.69	10.2	1.096
P-8,2	293	470.8	0.811	17.2	7489	1.04	1.38	12.46
	80	959.9	1.015	19.6	8426	11.2	13.3	0.795
O-3,3[8]	123	17.01	0.330	194	244.6	0.350	1.43	136
O-4,4[8]	123	19.0	0.97	510	321.8	0.258	7.1	72
M-4,4[8]	123	529	1.66	31.0	334.4	0.466	1.39	22.0
M-3,3[8]	123	812	3.77	4.64	160	0.48	1.96	2.4
HQ-5,5	293	925.5	0.301	3.25	1504	1.38	9.16	0.355
	80	1441	3.92	27.2	2209	5.34	24.2	1.126
HQ-6,6	293	3353	0.736	2.20	2599	2.62	10.1	0.217
	80	3964	1.361	3.43	3072	10.6	34.5	0.100
DiMeO-P-5,5	293	3690	0.424	1.15	5350	2.45	4.58	0.251
	80	916.1	0.444	4.85	4691	9.14	19.5	0.249
1,4-Naph-5,5	293	414.3	0.342	8.26	4727	6.92	14.6	0.564
	80	1733	0.366	2.11	8368	16.5	19.7	0.107

formational changes are sensitive to temperature variations, they should be manifested in the intra-EET yield. The temperature-dependent quantum yield measurements[22] (Figure 8 and Tables III and IV) show that intra-EET is more efficient at higher temperatures, indicating a temperature-activated process. The kinetic model suggested for describing this temperature-dependent intra-EET process in bichromophoric molecules assumes[7] the following points.

(1) There are two conformations, $[D-(\ )-A]_1$ and $[D-(\ )-A]_2$, for the bichromophoric molecule D-( )-A for which the free energy difference is ΔE. The equilibrium constant for this conformational change is

$$K = \exp(-\Delta E/RT) \tag{13}$$

This assumption is supported by our molecular mechanics calculations, which indicate the existence of several stable conformations for the bichromorphic molecules of Figure 2.[19,20,22] These are approximated here by only two conformations.

(2) It is further assumed that the high-lying conformation is more favorable for intra-EET due to better orbital overlap. The two intra-EET rate constants for the two conformations, which are temperature independent, are $k_{ET}^{(1)}$ and $k_{ET}^{(2)}$, respectively.

The kinetic analysis of this model yields the following result for ϕ:[7d]

$$\phi^{-1} - \Phi_0^{-1} = \delta\phi_0^{-1}\tau_D k_{ET}^{(1)} \exp(-\Delta E/RT) \tag{14}$$

where

$$\delta = \tau_D k_{ET}^{(2)}/[\tau_D k_{ET}^{(1)}(1 + \tau_D k_{ET}^{(2)})] \tag{15}$$

τ_D is the actual fluorescence lifetime of D*, Φ_0 is the extrapolated value of ϕ at 0 K, and ϕ_0 is the quantum yield of the separate donor chromophore fluorescence in the absence of intra-EET.

(3) All of the observed temperature dependence may be attributed to the intra-EET activated process since no temperature dependence is observed for the separate D* molecule.[7,22,23]

The relation predicted by eq 14 was examined for all bichromophoric compounds, and the fit to eq 14 is shown in Figure 8 for P-7,3 with ΔE results summarized in Table III. Only for P-6,4 are there some deviations from the predicted temperature-dependent fluorescence yield (Figure 12). This may be attributed to the existence of an intramolecular exciplex or some other photoisomer whose emission was observed around 370 nm (Figure 13). Such an exciplex or photoisomer emission is observed for most bichromophoric compounds,[22] but it is rather pronounced for P-6,4 at low temperatures.

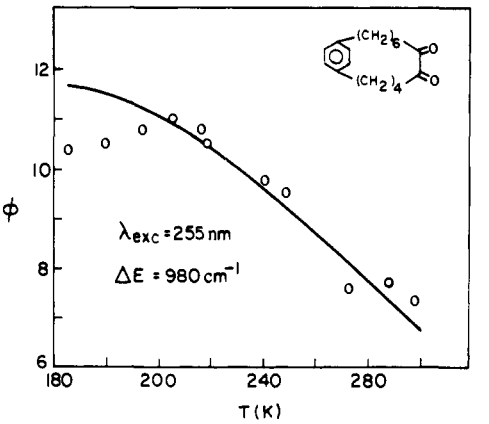

Figure 12. Temperature-dependent relative fluorescence quantum yield ϕ for the aromatic chromophore of the bichromophoric molecule P-6,4 together with the line fitted to eq 14.

Neglecting such an intramolecular exciplex or photoisomer emission, we related the temperature-dependent donor fluorescence quantum yield ϕ to the intra-EET quantum yield Q:

$$Q = 1 - \phi/\phi_0 \tag{16}$$

Table III summarizes the Q values and the corresponding ΔE values obtained from the fit to eq 14 or all bichromophoric compounds. The quality of the fit suggests that intramolecular exciplex or photoisomer formation is not that significant for the intra-EET process.

The range of ΔE values is typical of conformational changes in methylene bridges.[20] Different bridges give rise to different ΔE values since a difference in the relative orientations and positions of the α-diketone with respect to the aromatic ring requires different distortion to arrive at that conformation which facilitates the intra-EET process. Thus, for those compounds such as P-4,4, P-6,6, and O-3,3, for which molecular mechanics indicated the existence of only one stable conformation, temperature dependence for Q is not observed.[7]

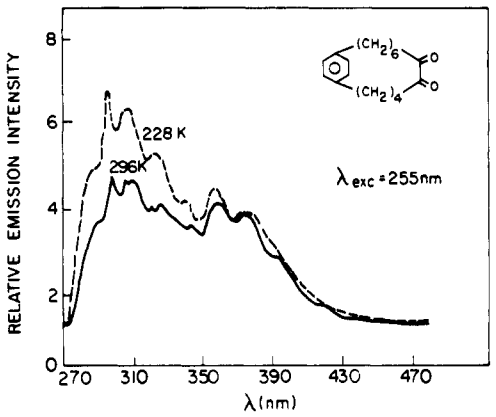

Figure 13. Fluorescence spectra for the bichromophoric molecule P-6,4 excited by 255 nm at two temperatures.

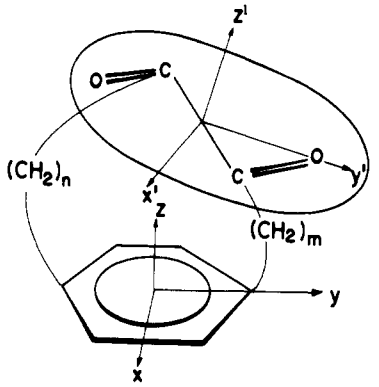

Figure 14. Coordinate systems of the bichromophoric molecule. The primary system xyz is of the aromatic ring, while the secondary system $x'y'z'$ is of the α-diketone.

The relation of ΔE to the spectral overlap integral J' is shown in Table IV. It is clear that a larger molecular distortion and therefore larger ΔE is required for molecules for which unfavorable spectral resonance conditions exist. However, the temperature dependence should also be related to the actual orbital overlap and the structure dependence of the intra-EET process, which is discussed in the next subsection.

4.2 Conformational Averaging and the Calculation of the Exchange Integral. For each given temperature we have observed structure-dependent Q, as is evident from examination of Figure 6 and Table III. The room-temperature results for Q together with the average interchromophore distance $\bar{R}$ are shown in Table III. It is evident that Q is a decreasing function of $\bar{R}$. This $\bar{R}$ dependence of Q can be calculated by assuming a certain spatial distribution for the conformations of the bichromophoric molecules. The molecular geometry for which this average is performed is shown in Figure 14.

The conformational dependence can be described by a distribution function $F(R, \theta', \phi')$ in the coordinate system suitable for the calculation of the exchange integral Z, shown in Figure 4 and 16. Using this distribution function, the average decay signal $\bar{P}(t)$ for the donor fluorescence is given by

$$\bar{P}(t) = \int \exp[(-t/\tau_D)(1 + \tau_D k_{ET}^{intra})] F(R,\theta',\phi')\, dR\, d\theta'\, d\phi' \quad (17)$$

The donor fluorescence quantum yield is then given by

$$\phi = k_r \int_0^\infty \bar{P}(t)\, dt \quad (18)$$

where k_r is the radiative decay rate of the donor moiety.

In order to calculate $\bar{P}(t)$, we have to assume a certain functional dependence for $F(R,\theta',\phi')$. Since the variations in R, θ', and ϕ' are independent, we can write

$$F(R,\theta',\phi') = F(R)F(\theta')F(\phi') \quad (19)$$

Thus,

$$\bar{P}(t) = \Theta\Phi \int \exp[(-t/\tau_D)(1 + \tau_D k_{ET}^{intra})] F(R)\, dR \quad (20)$$

where Θ and Φ are molecular geometry constants given by

$$\Theta = \int F(\theta')\, d\theta' \quad (21)$$

$$\Phi = \int F(\phi')\, d\phi' \quad (22)$$

For symmetrical bichromophoric molecules, we have assumed a symmetrical Gaussian distribution for $F(R)$:[7c,d]

$$F(R) = (\gamma/\pi)^{1/2} \exp[-\gamma(R - \bar{R})^2] \quad (23)$$

where γ is a temperature-dependent width which can be related to the temperature-dependent quantum yield measurements.

Using eqs 17–23, $\bar{P}(t)$ can be calculated to finally yield[7c,d]

$$\phi = \phi_0[1 - (\tau_D/\bar{\tau}) \exp(\beta^2/4\gamma)] \quad (24)$$

where

$$\phi_0 = \tau_D k_r \quad (25)$$

and

$$\bar{\tau} = \tau_D \exp[\beta(\bar{R} - R_0')] = \alpha^{-1} \exp(\beta\bar{R}) \quad (26)$$

Thus, for symmetrical bichromophoric molecules the intra-EET quantum yield (eq 16) is

$$Q = \exp(\beta^2/4\gamma) \exp(\beta R_0') \exp(-\beta\bar{R}) \quad (27)$$

or

$$Q = \tau_D \alpha \exp(\beta^2/4\gamma) \exp(-\beta\bar{R}) = \tau_D \bar{k}_{ET} \exp(\beta^2/4\gamma) \quad (28)$$

where

$$\bar{k}_{ET} = \alpha \exp(-\beta\bar{R}) \quad (29)$$

from which we obtain

$$Q' \equiv (Q/\tau_D\alpha) \exp(\beta^2/4\gamma) = \exp(-\beta\bar{R}) \quad (30)$$

which predicts a linear dependence of $\ln Q'$ vs $\bar{R}$ which can be tested experimentally. Deviations from linearity can be attributed to orientational effects not accounted for in eq 29 due to neglect of the θ' and ϕ' dependence in the conformational averaging and due to the simple Gaussian distribution used for $F(R)$ which should hold only for symmetrical bichromophoric molecular structures.

The $\exp(\beta^2/4\gamma)$ factor in eq 27 is related to the temperature-dependent quantum yield measurements in eq 14 through[7]

$$\exp(\beta^2/4\gamma) = 1 + \delta \exp(-\Delta E/RT) \quad (31)$$

which, for narrow conformational distributions in which $\gamma \gg 1$, reduces to

$$\gamma^{-1} = (4\delta/\beta^2) \exp(-\Delta E/RT) \quad (32)$$

It can be shown that this relationship fits a model in which the conformational changes involving the methylene bridge can be thought of as vibrational bending modes associated with the bridges, reflecting the flexibility of the bridge.[7c,d]

A recent calculation of the exchange integral[19] for molecules of the type depicted in Figure 2 allows us to relate the calculated Z value with the experimental Q' values. In the calculation, the molecular distortions are determined using the translation matrix of Figure 14 and combining it with the rotations depicted in Figure 15. In this way it was established that the main factor determining Z is R, with a smaller dependence on θ' and ϕ' and minor dependence on θ, ϕ, and χ. The fit of the experimental room-temperature Q' values obtained from the data of Tables III and IV to eq 30 is shown in Figure 16 together with the calculated Z values.[19] It is clear that a good fit is found for the symmetric bichromophoric molecules to the simple exponential dependence resulting from the Dexter relation eq 10. For all of these symmetrical bichromophoric molecules, the fit is to the same $L = 2.32$

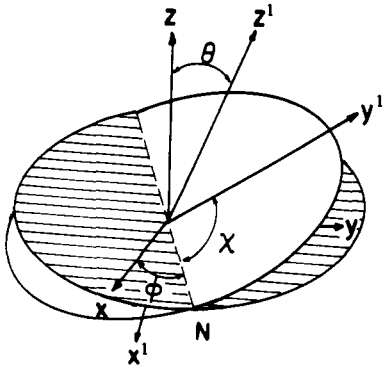

Figure 15. Description of the parameters in the rotation matrix of the plane of the α-diketone in relation to the plane of the aromatic ring. θ, ϕ, and χ are the Euler angles.

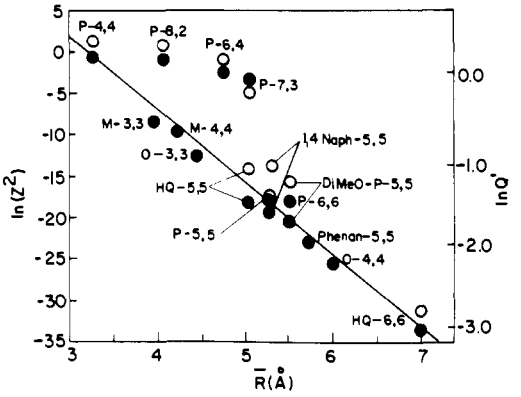

Figure 16. Plot of ln Q' vs $\bar{R}$ together with the calculated exchange integral (eq 7) showing the fit to eq 28.

Å value for the van der Waals radius. Deviations are observed for all asymmetric molecules where the relative orientation of the chromophores plays a role in determining Z, which is reflected in the poor fit of the Q' values to eq 30. However, even though the simple exponential $\bar{R}$ dependence does not hold, we still maintain the relation

$$Q' \propto Z^2 \tag{33}$$

which results from the combination of eqs 8, 12, and 16 and the definition of Q' in eq 30.

In our discussion we have ignored the possibility of through-bond interactions that may lead to superexchange promoting intra-EET over large $\bar{R}$ values.[11] We also did not consider higher multipole interactions that may play a role in systems with poor spectral overlap. While there is no simple way of evaluating such contributions to the observed Q' vs $\bar{R}$ data, the quality of the fit to eq 14 suggests that in our system intra-EET is mostly governed by exchange interaction.

4.3. Kinetic Analysis of Triplet–Triplet Intra-EET. In this subsection we correlate parameters obtained in time-resolved experiments (Figures 10 and 11)[22] with analysis of the kinetic scheme shown in Figure 17. Experimentally the acceptor emission spectra due to two excitation routes were recorded: that of direct excitation of the acceptor chromophore (the α-diketone at 430 nm) and that of separate excitation of the donor chromophore (benzene ring at 266 nm). The latter route must involve intra-EET. Relative yields of emissions were obtained from integration of the time-resolved bands.

The excitation processes, emission processes, and various radiationless decay routes of the bichromophoric molecules are summarized in the kinetic scheme of Figure 17. Excitation at 266 nm prepares a $\pi\pi^*$ singlet state (S_1^D) of the aromatic chromophore which either undergoes an intersystem crossing process (k_{ISC}^D) to triplet $\pi\pi^*$ or prepares the $\pi\pi^*$ singlet state of the α-diketone (k_{ET}^{S-S}). In solution this state decays in a nonradiative fashion to the single $n\pi^*$ of the α-diketone; both states are denoted here together as S_1^A. A spin–orbit interaction couples both these

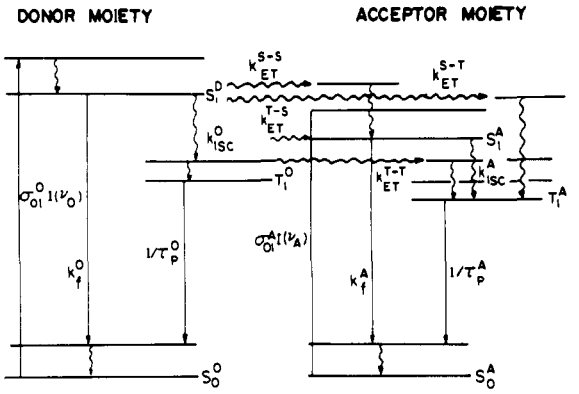

Figure 17. Schematic energy level diagram for describing S-S, S-T, and T-T intra-EET in a donor–acceptor bichromophoric molecule. The donor (D) or the acceptor (A) chromophores can be excited separately by choosing the corresponding excitation frequency, ν_A or ν_D, respectively; the excitation rates are $\sigma_{01}^A(\nu_A)$ and $\sigma_{01}^D(\nu_D)$ where σ_{01} denotes the corresponding absorption cross sections and I the exciting laser intensity. k_{ET} denotes intra-EET rates, k_{ISC} denotes ISC rates, k_f is the sum of $S_1 \rightarrow S_0$ decay rates, and τ_P's are the corresponding phosphorescence lifetimes.

acceptor singlet states to the acceptor $n\pi^*$ (k_{ISC}^A process). In fact, one would expect the coupling between the acceptor singlet $^1\pi\pi^*$ and its $^3n\pi^*$ triplet to be more significant than the $^1n\pi^* \rightarrow {}^3n\pi^*$ process. Kinetically, however, we simplify the discussion by assuming a single ISC rate constant.

For direct excitation at 430 nm, the situation is simpler since here the singlet $n\pi^*$ state of the α-diketone is prepared ($\sigma_{01}^A I$ process) and k_{ISC}^A is the $^1n\pi^* \rightarrow {}^3n\pi^*$ rate constant. Our results indicate that k_{ISC}^A depends to a large extent on the molecular geometry (see below), and this effect is much more significant in comparing the direct excitation route to acceptor triplet preparation by intra-EET than the relative contributions of $\pi\pi^*$ and $n\pi^*$ singlet states to k_{ISC}^A.

The fluorescence and phosphorescence data are summarized in Table VI in terms of the following parameters:

$$\rho_d \equiv \phi_P^d(A)/\phi_F^d(A) = \tau_A k_{ISC}^A \phi_P^o(A)/\phi_F^o(A) \tag{34}$$

$$\rho_{ET} \equiv \phi_P^{ET}(A)/\phi_F^{ET}(A) = [\tau_A k_{ISC}^A(Q_{ET}^{S-S} + Q_{ET}^{T-S}) + Q_{ET}^{S-T} + Q_{ET}^{T-T}]\phi_P^o(A)/(Q_{ET}^{S-S} + Q_{ET}^{T-S})\phi_F^o(A) \tag{35}$$

$$\xi^{T-T} \equiv \rho^{ET}/\rho^d = 1 + (Q_{ET}^{S-T} + Q_{ET}^{T-T})/(Q_{ET}^{S-S} + Q_{ET}^{T-S})\tau_A k_{ISC}^A \tag{36}$$

where the superscript d denotes direct excitation of the acceptor chromophore at 430 nm and the superscript ET denotes the intra-EET excitation route of the acceptor following excitation of the donor at (266 nm) (see Figure 17). The ratios ρ are obtained from the measured fluorescence and phosphorescence relative quantum yields of the acceptor $\phi_F(A)$ and $\phi_P(A)$, respectively, $\phi_P^o(A)$ and $\phi_F^o(A)$ are the corresponding absolute quantum yields, and τ_A is the acceptor's fluorescence lifetime. The various intra-EET quantum yields are denoted Q_{ET} with suitable superscripts. The triplet–triplet intra-EET process is expressed in terms of the parameter ξ^{T-T}, defined in eq 36. The existence of singlet–triplet and triplet–triplet intra-EET routes in addition to direct excitation routes of the acceptor triplet is manifested in $\xi^{T-T} > 1$.

The results for $\phi_F(A)$ (Table VI) were corrected for the amount of fluorescence resulting from direct excitation of the α-diketone moiety at 266 nm. This was accomplished by using $\phi_F(A)$ of O-4,4, for which $Q_{ET}^{S-S} = 0.02$,[5] as a reference whose fluorescence excited at 266 nm is due mainly to direct excitation of the α-diketone moiety. In doing so, we neglect contribution from the direct triplet–singlet intra-EET route for O-4,4. Inspection of Table VI reveals that $\xi^{T-T} > 1$ for the P-*n*,*m* series in accordance with previous observations made on P-*n*,*n*, O-*n*,*n*, and M-*n*,*n* bichromophoric molecules.[6] The results for all other molecules

indicate that additional decay routes, not included in the present analysis, play a significant role in the process. For example the observation of intramolecular exciplex fluorescence emission is a manifestation of a decay route. In addition, the correction procedure based on the O-4,4 standard is likely to fail for compounds other than the P-*n,m* series for which direct excitation of acceptor fluorescence at 266 nm cannot be neglected. For those compounds for which $\xi^{T-T} > 1$, we expect to observe complementarity between singlet–singlet intra-EET and triplet–triplet intra-EET. Only P-8,2 deviates from this general behavior. This can be understood since for P-8,2 the interchromophoric distance is shorter than that for the other molecules of the P-*n,m* series, promoting both modes of intra-EET.

While the above analysis shows the existence of the triplet–triplet intra-EET process, it is incomplete. It does not reveal the exact structural dependence of triplet–triplet intra-EET in bichromophoric molecules. For singlet–singlet intra-EET we were able to demonstrate that the Dexter[18] exchange interaction can serve as a good approximation for the mechanism of this process. Since triplet–triplet intra-EET is usually described by the same mechanism, Q_{ET}^{T-T} should be expressed in a form similar to eq 30. Yamamoto and co-workers have shown recently[25] that indeed this is the case for a different series of bichromophoric molecules. In their series,[25] the triplet–triplet intra-EET process could be evaluated by following the intramolecular quenching of the donor chromophore phosphorescence. Unfortunately, due to the negligible phosphorescence of the aromatic chromophore in our series of compounds, such an approach could not be applied.

(25) Katayama, H.; Maruyama, S.; Ito, S.; Tsujii, Y.; Tsuchida, A.; Yamamoto, M. *J. Phys. Chem.* **1991**, *95*, 3480.

5. Conclusions

We have shown that exchange interaction controls short-range intramolecular electronic energy transfer in bichromophoric molecules for which the spectral overlap integral is low. Special design of bichromophoric molecular structure made it possible to determine the contributions of interchromophore distance and relative chromophore orientation to exchange interaction. It is concluded that in general the exchange integral and singlet–singlet intra-EET are dependent upon the relative orientation of the interacting orbitals, resulting in a preferred orientation for electron exchange. However, the simple Dexter formulation of exchange interaction still holds in some cases.

In addition, we have demonstrated the triplet–triplet intra-EET process in bichromophoric molecules. This process complements our observation of singlet–singlet intra-EET. In contrast to singlet–singlet intra-EET, complete quantitative analysis of the structural dependence of this process requires the separation of the singlet–singlet and triplet–triplet routes from the intersystem crossing processes. Thus, the complete molecular structural dependence of the triplet–triplet intra-EET process was not established for our series of bichromophoric molecules.

Acknowledgment. This study was supported in part by a grant (No. 84-00391) from the U.S.–Israel Binational Science Foundation.

Flavin-Photosensitized Monomerization of Dimethylthymine Cyclobutane Dimer: Remarkable Effects of Perchloric Acid and Participation of Excited-Singlet, Triplet, and Chain-Reaction Pathways

Chyongjin Pac,*,† Kunihito Miyake,‡ Yasuhiro Masaki,‡ Shozo Yanagida,‡ Takeshi Ohno,§ and Akio Yoshimura§

Contribution from Kawamura Institute of Chemical Research, Sakado, Sakura, Chiba 285, Japan, Department of Chemical Process Engineering, Faculty of Engineering, Osaka University, Suita, Osaka 565, Japan, and Chemistry Department, College of General Education, Osaka University, Toyonaka, Osaka 560, Japan. *Received June 22, 1992*

Abstract: We report the efficient monomerization of the cis-cisoid cyclobutane dimer of 1,3-dimethylthymine photosensitized by riboflavin tetraacetate (r-Fl), 3-methyl-8-chloro-10-phenyl-5-deazaflavin (d-Fl), and lumiflavin in acetonitrile in the presence of $HClO_4$, as a model reaction of photorepair. The limiting quantum yields are unity for the r-Fl-photosensitized monomerization in degassed and aerated solution and also for the d-Fl-photosensitized run in degassed solution. Mechanistic studies involving kinetic analysis of the reactions, fluorescence quenching, and laser-flash photolysis demonstrate that the photosensitized monomerization proceeds through electron transfer from the dimer to the protonated flavins in both the excited-singlet and triplet states. It is suggested that the singlet and triplet radical pairs initially formed by the electron transfer exclusively undergo the net monomerization with little participation of geminate recombination back to the precursors. A chain reaction has been found to participate as another mechanistic channel in the r-Fl-photosensitized monomerization of Ar-purged solution and in the d-Fl-photosensitized reaction of Ar-purged and aerated solution; the limiting quantum yields are much greater than unity. It is suggested that a chain carrier is photochemically generated from the protonated form of r-Fl or d-Fl to catalyze the monomerization of the dimer complexed with O_2.

Introduction

The ultraviolet (UV) induced cyclodimerization of pyrimidine bases in DNA is a major origin of lethal and/or mutagenic UV effects of biological systems,[1] which can be repaired upon exposure of UV-irradiated biological systems to near-UV and/or visible light.[1,2,3a] The photorepair of UV-damaged DNA requires enzyme

† Kawamura Institute of Chemical Research.
‡ Faculty of Engineering, Osaka University.
§ College of General Education, Osaka University.

(1) Cadet, J. In *Bioorganic Photochemistry*; Morrison, H., Ed.; John Wiley & Sons: New York, 1990; Vol. 1, pp 1-272.
(2) Sancar, A.; Sancar, G. B. *Ann. Rev. Biochem.* **1988**, *57*, 29.

0002-7863/92/1514-10756$03.00/0